Oscillation Characteristics of Biofilm Streamers in Turbulent Flowing Water as Related to Drag and Pressure Drop

Paul Stoodley,[1] Zbigniew Lewandowski,[2] John D. Boyle,[3] Hilary M. Lappin-Scott[1]

[1]Environmental Microbiology Research Group, University of Exeter, Department of Biological Sciences, Hatherly Laboratories, Exeter, Devon EX4 4PS, United Kingdom; telephone: 44 1392 264348; fax: 44 1392 263700; e-mail: P.Stoodley@exeter.ac.uk
[2]Center for Biofilm Engineering, 407 Cobleigh Hall, Montana State University, Bozeman, Montana 59717
[3]University of Exeter, School of Engineering, North Park Road, Exeter, Devon EX4 4QF, United Kingdom

Received 9 May 1997; accepted 5 August 1997

Abstract: Mixed population biofilms consisting of *Pseudomonas aeruginosa, P. fluorescens,* and *Klebsiella pneumoniae* were grown in a flow cell under turbulent conditions with a water flow velocity of 18 cm/s (Reynolds number, Re, =1192). After 7 days the biofilms were patchy and consisted of cell clusters and streamers (filamentous structures attached to the downstream edge of the clusters) separated by interstitial channels. The cell clusters ranged in size from 25 to 750 µm in diameter. The largest clusters were approximately 85 µm thick. The streamers, which were up to 3 mm long, oscillated laterally in the flow. The motion of the streamers was recorded at various flow velocities up to 50.5 cm/s (Re 3351) using confocal scanning laser microscopy. The resulting time traces were evaluated by image analysis and fast Fourier transform analysis (FFT). The amplitude of the motion increased with flow velocity in a sigmoidal shaped curve, reaching a plateau at an average fluid flow velocity of approximately 25 cm/s (Re 1656). The motion of the streamers was possibly limited by the flexibility of the biofilm material. FFT indicated that the frequency of oscillation was directly proportional to the average flow velocity ($u_{(ave)}$) below 9.5 cm/s (Re 629). At $u_{(ave)}$ greater than 9.5 cm/s, oscillation frequencies were above our measurable frequency range (0.12–6.7 Hz). The oscillation frequency was related to the flow velocity by the Strouhal relationship, suggesting that the oscillations were possibly caused by vortex shedding from the upstream biofilm clusters. A loss coefficient (k) was used to assess the influence of biofilm accumulation on pressure drop. The k across the flow cell colonized with biofilm was 2.2 times greater than the k across a clean flow cell. *Biotechnol Bioeng* **57:** 536–544, 1998.
Keywords: biofilm; streamers; biofouling; drag; fast Fourier transform analysis; hydrodynamics; oscillations; pressure drop

Correspondence to: P. Stoodley
Contract grant sponsors: National Science Foundation/Montana State University and Exeter University.
Contract grant number: EEC-8907039

INTRODUCTION

Biofilms growing in pipelines can result in increased fluid frictional resistance and reduced flow capacity (Bryers and Characklis, 1981). Research by Picologlou et al. (1980) found that the fouling biofilm caused a greater pressure drop across a tubular flow cell than would be expected if the biofilm were rigid. They hypothesized that this was due to the viscoelasticity and filamentous nature of the biofilm. Previously, Characklis (1979) concluded that biofilms caused an increase in pressure drop only when the thickness of the biofilm had reached that of the theoretical thickness of the viscous sublayer. The implication is that the viscous sublayer remains unaffected during biofilm development until a certain critical thickness is reached. McCoy and Costerton (1982) suggested that the pressure drop increased when the length of the filaments had reached the theoretical thickness of the viscous sublayer, assuming that the filaments were protruding away from the wall through the viscous sublayer. This assumption may have arisen from the methods they used to observe the biofilm: coupons were removed from the flow cell and observed under static conditions using SEM and fluorescence microscopy. Thus, information concerning the orientation and behavior of the filaments in the flowing water was lost. Although both of these observations may be empirically useful, they do not elucidate the mechanisms of interactions between the biofilm and the flowing water.

The overall pressure drop (or friction factor) is influenced by two principal phenomena: skin friction and pressure (or form) drag (Vogel, 1994). Skin friction is dominant at low viscous flows and is strongly influenced by surface area. Pressure drag is dominant at high turbulent flows and is chiefly a function of the shape, size, and rigidity of the body. Therefore, in laminar flow it is the total surface area of the biofilm that will possibly have the greatest influence on pressure drop, but in turbulent flow it is the shape of the

 CCC 0006-3592/98/050536-09

biofilm structures that will be the significant factor. Three types of flow regimes have been identified for flow over rough surfaces (Nowell and Church, 1979). When surface protrusions (sometimes termed ''roughness elements'') cover much of the surface, there is a ''skimming flow'' in which the velocity profile is vertically relocated to the top of the surface protrusions. When surface protrusions cover only a small proportion of the surface, an ''isolated roughness flow'' occurs in which there is little interaction between wakes from the protrusions and only a small influence on the velocity profile. Between these extremes a ''wake interaction flow'' occurs in which the downstream protrusions experience unsteady flow from the wakes shed by the upstream protrusions. Nowell and Church (1979) found that the greatest resistance to flow occurred when there was skimming flow at a surface roughness coverage of 1/12. Most of the studies on flow over rough surfaces have been done using uniform rigid protrusions. Flow over flexible, nonuniform, randomly spaced surface protrusions, such as occur in heterogenous biofilms, will almost certainly add greater degrees of complexity.

In previous work on hydrodynamic influences on biofilms grown under laminar flow, we reported the formation of heterogenous biofilms consisting of cell clusters (aggregates of bacterial cells in a slime matrix) separated by interstitial channels (deBeer et al., 1994a). Using particle tracking techniques, we were able to document the existence of water flow in the channels (Stoodley et al., 1994). Velocity profiles measured in the biofilms indicated that there was a transition from hydrodynamically smooth flow to rough flow when the roughness Reynolds number [Re_r, introduced by Nikuradse in 1933 and described in detail by Characklis et al. (1990) and Jumars and Nowell (1984)] was greater than 5 (deBeer et al., 1994b). This was close to reported values that show that the transition between smooth and rough flow occurs at $Re_r > 3.5$ (Characklis et al., 1990; Jumars and Nowell, 1984).

We extended our investigations to biofilms growing under turbulent conditions, which are hydrodynamically more relevant to many industrial pipeline systems than laminar flows. We designed a flow cell that could be mounted onto the stage of a confocal laser scanning microscope (CSLM) that allowed the biofilm to be observed in situ under flow conditions (Lewandowski and Stoodley, 1995). The biofilm structure was significantly different under high flow. The biofilm developed filamentous structures similar to those described by other researchers using turbulent conditions (Bryers and Characklis, 1981; Characklis, 1979; McCoy and Costerton, 1982; McCoy et al., 1981; Picologlou et al., 1980). The filaments had complex structures and appeared to be formed from the colonization of individual filaments by microcolonies. We termed the filaments ''streamers'' to distinguish them from filamentous sheathed bacteria or bacterial chains. The streamers were attached to the downstream side of the cell clusters and were free to oscillate in the flowing water. We hypothesized that the oscillation of the streamers was caused by vortex shedding from the clusters. However, we did not have a method for quantifying the motion of the streamers.

The goal of this research was to observe the formation of biofilm streamers over time under flowing conditions and quantitatively describe the oscillatory motion of the streamers at different flow velocities. We wished to further investigate our hypothesis that the streamer movement was caused by vortex shedding by relating the streamer oscillation frequency to the flow velocity, a well established relationship in hydrodynamics described by the dimensionless Strouhal number (Vogel, 1994). We had three objectives: to design a flow cell that would allow biofilms grown in turbulent flow to be microscopically examined in situ by CSLM so that streamer motion could be recorded; to determine the relationship between flow velocity and streamer motion; and to relate biofilm formation and streamer motion to pressure drop. We used a loss coefficient (k) as a comparative measure of biofouling. The loss coefficient is commonly used by engineers to determine energy losses across different pipe fittings (Massey, 1979).

MATERIALS AND METHODS

Reactor System and Microscopy

The reactor system consisted of a flow cell incorporated into a recycle loop with a mixing chamber for aeration and nutrient addition. The flow cell was a polycarbonate channel (0.5 cm wide, 1 cm deep, and 24 cm long) with a rectangular coverslip viewing port (60 × 24 mm) sealed with a rubber gasket and an aluminum flange. The flow cell could be placed on the stage of an inverted microscope (Olympus IMT-2) attached to a Bio-Rad MRC600 CSLM. A differential pressure transducer (Foxboro Co., model 843DP-H1V1NK, Foxboro, MA) was used to monitor the pressure drop across the flow cell. The pressure transducers were calibrated with a mercury manometer. Tee fittings connected to the inlet and outlet flow cell tubing (3 cm on either side of the flow cell inlet and outlet) were used as pressure ports. The distance between the pressure ports was 30 cm. The measured pressure drop, therefore, included expansion and contractions between the tee fittings and the connecting tubing, the flow cell and the connecting tubing, and bends in the tubing that were required to position the flow cell on the CSLM stage. Once the flow cell was positioned on the stage, it was not disturbed during the experiment. Nutrients and dilution water were delivered by a peristaltic pump (Masterflex, Cole Parmer, Niles, IL), and the recycle flow rate (Q_R) was controlled using a vane head pump and measured with an in-line flow meter (McMillan Flo-sensor model 101T supplied by Cole–Parmer, Niles, IL). The flow meter was calibrated by volumetric displacement. The average flow velocity ($u_{(ave)}$) in the flow cell was found by dividing the flow rate by the cross-sectional area of the flow cell. The nutrients were mixed with the dilution water in a ratio of 1:9 (2 mL/min:18 mL/min) for a final concentration

of glucose at 40 ppm, potassium phosphate monobasic (KH_2PO_4) at 70 ppm, potassium phosphate dibasic (K_2HPO_4) at 30 ppm, ammonium sulfate [$(NH_4)_2SO_4$] at 10 ppm, and magnesium sulfate ($MgSO_4 \cdot 7H_2O$) at 1 ppm. The volume of the mixing chamber and recycle loop, including the flow cell, was 400 mL. A combined influent (nutrients and dilution water) flow rate of 20 mL/min was chosen to give a hydraulic residence time in the complete system of 20 min so that suspended cells would be washed out and biofilm growth was favored. The volume in the recycle loop (pump, tubing, and flow cell) was approximately 250 mL. The flow rate in the recycle loop was 9 mL/min, resulting in a hydraulic residence time of 22 s. Because the residence time in the recycle loop was very small, we assumed that the system was well mixed.

Flow Cell Hydrodynamics and Determination of Loss Coefficient (*k*)

The Re in the flow cell was found from

$$\mathrm{Re} = \frac{u_{(\mathrm{ave})} D_\mathrm{h}}{\nu}, \tag{1}$$

where D_h was the hydraulic diameter and ν was the kinematic viscosity of water (1.007×10^{-6} m^2/s at 20°C). D_h (0.667 cm) was based on the cross-sectional area and wetted perimeter (Lewandowski et al., 1995). The flow cell was 36 entrance (hydraulic) diameters in length, and the viewing area was positioned between 20 and 22 entrance diameters from the inlet.

We wished to operate the flow cell under turbulent conditions and used the relationship between pressure drop (ΔP) and $u_{(ave)}$ to characterize the hydrodynamics in the flow cell. ΔP is related to $u_{(ave)}$ according to

$$\Delta P = \frac{k u_{(\mathrm{ave})}^{\ m} \rho_\mathrm{w}}{2}, \tag{2}$$

where k is the coefficient of proportionality referred to as the loss coefficient, m is a dimensionless coefficient dependent on pipe roughness, and ρ_w is the density of water (998 kg/m^3 at 20°C) (Massey, 1979). Under turbulent conditions m is 1.75 for smooth pipes and 2 for rough pipes (Kay, 1957). The pressure drop was measured at various $u_{(ave)}$ over the entire pump range (0–60.2 cm/s, Re 0–3987) in a clean flow cell and then monitored daily during biofilm growth. After a 7-day growth period the pressure drop was measured again over the achievable pump range of $u_{(ave)}$ (0–51 cm/s, Re 0–3377). The k and m values were found for the flow cell before and after biofilm accumulation by linear regression of the $\log_{10} \Delta P - \log_{10} u_{(ave)}$ curves.

Sterilization and Inoculation

The flow cell, mixing chamber, and recycle tubing were sterilized by exposure to a 1% household bleach solution for 24 h. The bleach was removed by rinsing with about 70 vol aerated filter-sterilized tap water, 3 vol sterile sodium thiosulfate (100 ppm), and finally about 70 vol aerated filter-sterilized tap water. Tap water was used for nutrient dilution. Chlorine was removed by air sparging and an in-line activated charcoal column. The dilution water was sterilized with in-line capsule filters (1.0-μm prefilter and 0.1-μm filter). The nutrient feed and associated tubing were sterilized by autoclaving at 121°C for 15 min. The mixing chamber was inoculated with stock cultures (1 mL) of *Pseudomonas aeruginosa*, *P. fluorescens*, and *Klebsiella pneumoniae*. The concentration of cells in the stock cultures was between 10^{10} and 10^{11} cells/mL (Stoodley et al., 1994). The reactor system was initially run as a batch culture for 12 h to ensure attachment before switching to continuous culture. During the inoculation and growth phases, Q_R was maintained at 5.46 mL/min with a corresponding $u_{(ave)}$ of 18 cm/s (Re 1192). Flow was turbulent at this velocity (see the Results Section). The biofilm was grown for 7 days, and under operating conditions the temperature of the water in the system was 20 ± 1°C.

Biofilm Thickness Measurement

The biofilm thickness (dimension in the plane perpendicular to the substratum) is defined in this study as the distance between the substratum and the peaks of the highest cell clusters. Using this definition, the channels (void fraction) and the cell clusters and streamers (biomass fraction) were both considered integral components of the biofilm. The height of the biofilm cell clusters was measured microscopically by focusing on the substratum (glass coverslip) and then moving the stage a known distance with a stepper motor until the surface of the biofilm came into focus. Calibration of the stage stepper motor was required because the distance traveled by the stage was not the same as the distance between corresponding focal planes in the flow cell due to refraction by the air, glass, and water interfaces. The microscope was focused on the lower channel wall and then refocused on the upper channel wall (an actual distance of 1 cm) using the stepper motor, and the distance of travel was recorded. The ratio of actual distance to the traveled distance was used to determine the correction factor (1.359). The distance traveled by the stage relative to the glass substratum was multiplied by 1.36 to find the height dimension.

Streamer Motion

The path of motion of the streamers was visualized by staining the biofilm with neutral density fluorescent latex spheres (0.282-μm diameter, Molecular Probes, Eugene, OR). The spheres were added to the flow cell to achieve a final concentration of approximately 1×10^7 particles/mL. Some of the spheres attached to the streamers. Time exposed fluorescent images were taken to show the range of streamer motion.

Streamer Displacement Measurements

After the 7-day growth period, time trace images showing the motion of a biofilm streamer were captured with transmitted CSLM. The time traces were made at 20 different $u_{(ave)}$ from 0 to 50.5 cm/s (Re 0–3344), using the line scan function of the Bio-Rad COMOS operating system. A line on the screen that crossed a streamer was selected and scanned repeatedly. As the lines were scanned they were placed consecutively on the screen to build a full image (512 lines) in which the *X* axis represented distance (2.46 mm) and the *Y* axis time (25.6 s). In this way a time trace record was built up and the streamer appeared as a dark section in the line against the lighter background.

Image Analysis

Image analysis was used to measure biofilm length dimensions, surface coverage, and streamer oscillation characteristics. Processing was done on a Macintosh 7200/90 computer using the public domain NIH-Image 1.59 program (developed at the National Institutes of Health and available from the Internet by anonymous FTP from zippy.nimh.nih.gov or a floppy disk from the National Technical information service, Springfield, VA, Part PB95-500195GEI). Length and area measurements were calibrated using a 1-mm graticule with 10-μm divisions (ref. no. CS990, Graticules Ltd., Tonbridge, Kent, U.K.).

Biofilm Dimensions and Surface Coverage

The surface coverage of four fields of view (43.2 mm^2) were measured by applying a threshold so that the biofilm features (cell clusters and streamers) were black and the surrounding channels white. The relative surface coverage of the biofilm was the proportion of black to the total area. At the magnification used in this study, only the biofilm cell clusters, not the single cells on the glass surface, were included in the measurement.

Plan dimensions (in a plane parallel to the substratum) of biofilm cell clusters and streamers were measured using the ''line tool'' function that measures the distance between two points in an image.

Streamer Oscillation Wave Analysis

The oscillation time trace data were analyzed for wave frequency using fast Fourier transform analysis (FFT) with a commercial software package (Quattro Pro 6.0 for Windows, Novell Inc.). Before FFT could be performed, the time and displacement coordinates had to be extracted from the images. Thresholding was used, so that the streamers appeared as black sections in the white background line. A modification of the NIH-Image ''line plot → data'' macro (also available from the NIH-Image site) was used to find the center point of each of the biofilm line sections. The *XY* pixel coordinates were then converted to distance (μm) and time (s) using the appropriate scales. The average position of the streamer on the *X* axis was found and the maximum amplitude (half the total displacement) of the streamer was estimated by calculating the difference between the 3 standard deviations (incorporating 99% of data) from the mean. The data was smoothed using a 3-point moving average before performing FFT analysis.

RESULTS

Flow Cell Hydrodynamics before Biofilm Colonization

The pressure drop (ΔP) across the clean flow cell increased from 0.3 kPa when $u_{(ave)} = 3.8$ cm/s (Re 252) to 28.6 kPa when $u_{(ave)} = 60.2$ cm/s (Re 3987), the maximum pump output (Fig. 1). Above $u_{(ave)}$ of 10 cm/s (Re 662), ΔP was proportional to the 1.84 power of $u_{(ave)}$, indicating that flow was turbulent in this region. The loss coefficient (k) was 145 ($r^2 = 1.000$, $n = 17$).

Biofilm Growth

After 7 days growth at a $u_{(ave)}$ of 18 cm/s (Re 1192), the biofilm consisted of a patchy mosaic of cell clusters and streamers separated by channels (Fig. 2A,B). The surface coverage of the biofilm cell clusters was 41.8% (standard error = 2.1, $n = 4$). The cell clusters were roughly circular when viewed from above and ranged in size from 25 to 750 μm in diameter. The largest cell clusters were approximately 85 μm thick and had developed streamers that trailed from the downstream edge. The streamers were roughly conical in shape and tapered to a point in the down-

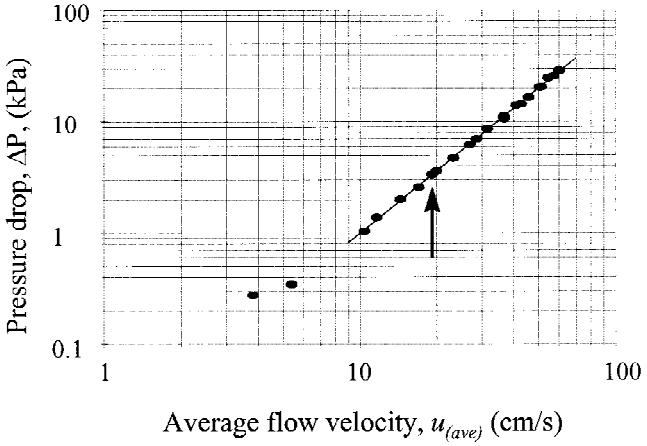

Figure 1. Relationship between pressure drop (ΔP) and average flow velocity ($u_{(ave)}$) for a clean flow cell. The closed circles are measured data. The solid line is the regression line calculated from data above 10 cm/s and indicates the turbulent region of the curve. The gradient of the regression line (1.84) is the velocity exponent, m in Eq. (2). The biofilm was grown at a flow velocity of 18 cm/s (shown by arrow).

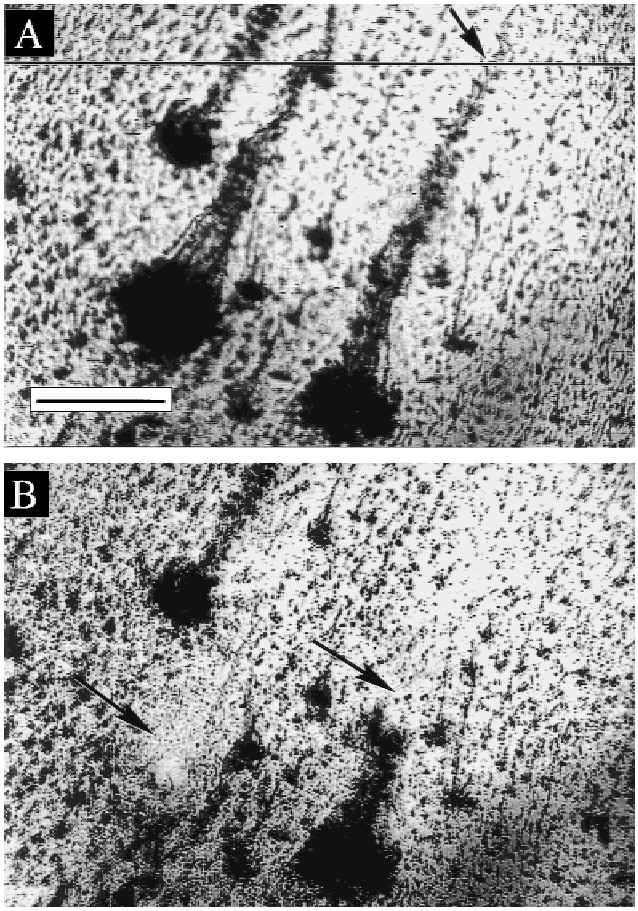

Figure 2. (A) Transmitted CSLM image showing biofilm clusters and streamers after 7-day growth. The horizontal black line indicates the position of the line scan used to make the time–displacement traces for subsequent wave analysis. The time traces used for analysis were made by the streamer intersecting the scan line shown by the arrow. Bulk flow was from bottom left to top right. (B) Sloughing of the biofilm occurred when the flow velocity was increased to 50.5 cm/s. A large cluster with a streamer was completely removed (left arrow), but small pieces of biofilm remained attached to the glass surface. One streamer broke off at about a third of the way along its length (right arrow). Images were enhanced for clarity using the equalize function in the NIH-Image software package. Scale bar = 500 μm.

stream direction. The streamers were up to 3 mm in length. The streamers formed a sinusoidal shape and oscillated from side to side (in the *X–Y* plane parallel to the channel wall) in the flow. Fluorescent beads attached to the streamers described arc paths in the time exposure images (Fig. 3). The streamer remained well focused during the observations, indicating that there was no significant motion perpendicular to the channel wall (*Z* plane). From the measurements of cell cluster thickness we estimated that the field of depth of our microscope setup was approximately 20 μm. Therefore, any displacement of the streamers in the *Z* plane was less than 20 μm.

The ΔP across the flow cell increased in a sigmoidal curve from 5.8 to 8.2 kPa after 89 h of biofilm accumulation (data not shown). The ΔP then leveled off and was 8.1 kPa at the end of the 7-day growth period.

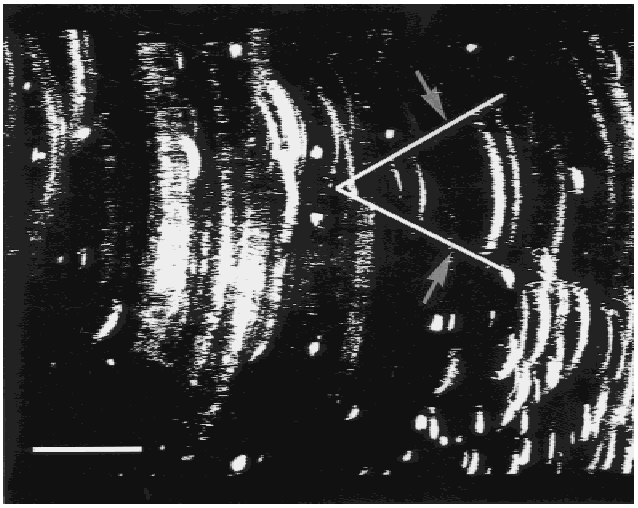

Figure 3. Time exposed image of fluorescent beads attached to biofilm streamers show the oscillating streamers formed arc shaped paths. The two white lines (shown by arrows) indicate the maximum displacement envelope (twice the maximum amplitude) of one of the streamers. Flow direction was from left to right. Scale bar = 500 μm.

Flow Cell Hydrodynamics after Biofilm Colonization

The ΔP increased from 0.35 kPa at a $u_{(ave)}$ of 2.4 cm/s (Re 159) to 45 kPa at a $u_{(ave)}$ of 50.5 cm/s (Re 3344) in the biofilm colonized flow cell (Fig. 4). For $u_{(ave)}$ greater than 10 cm/s (Re 662), the velocity exponent (m) was 1.86 and the k was 319 ($r^2 = 0.999$, $n = 20$). The maximum achievable flow rate in the reactor after biofilm colonization was 16% less than before biofilm growth. Some biofilm sloughing was noted at the maximum $u_{(ave)}$ of 50.5 cm/s. The corresponding shear stress (τ_w) at the wall of the flow cell was 1.32 N/m^2 from (McCabe and Smith, 1976)

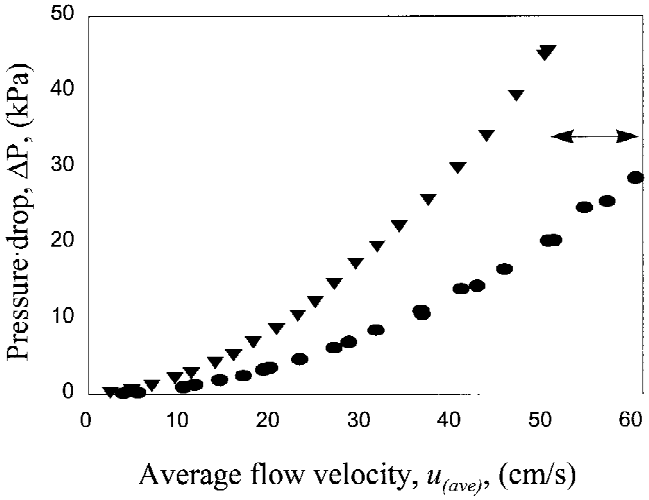

Figure 4. Relationship between pressure drop and flow velocity for a clean flow cell (circles, same data shown in Fig. 1) and for a flow cell colonized with biofilm (triangles). Biofilm colonization in the flow system resulted in a 16% decrease of achievable flow rate (indicated by the arrow).

$$\tau_w = \frac{f\rho_w u_{(ave)}^2}{2}, \quad (3)$$

where f is the Fanning friction factor,

$$f = \frac{0.0791}{Re^{0.25}}. \quad (4)$$

Some of the larger cell clusters and streamers were removed completely, but thin patches of biofilm were seen underneath (Fig. 2B). Other clusters remained attached, but their associated streamers had detached. Some of the streamers broke off near the edge of the cluster, but others broke further along the streamer.

Biofilm Streamer Movement

The displacement of the streamers increased with increasing $u_{(ave)}$ (Fig. 5). The FFT analysis provided a power spectrum (amplitude vs. frequency) data set for each of the 20 flow rates. The range of detectable frequencies was limited (0.12–6.7 Hz) by the sampling rate (0.05 lines/s), the data record length (512 lines), and data smoothing (3-point moving average). Generally the highest amplitudes occurred at the lower frequencies and amplitudes decreased exponentially toward zero at the higher frequencies (Fig. 6). Isolated amplitude peaks were identified by eye. Above $u_{(ave)}$ of 9.5 cm/s, there was a lot of fluctuation in the data and isolated peaks were not discernible. Below $u_{(ave)}$ of 9.5 cm/s, there was less fluctuation and peak identification was possible. Well defined amplitude peaks occurred at 0.78, 2.8, and 4.2 Hz at $u_{(ave)}$ of 1.2, 4.7, and 6.9 cm/s, respectively. The corresponding frequency (F) to flow velocity ratios ($F:u_{(ave)}$) of these peaks were 0.65, 0.60, and 0.64 cm^{-1} (Fig. 6, Table I). There were also isolated peaks of 4.3 Hz at $u_{(ave)}$ = 1.2 cm/s and 2.5 Hz at $u_{(ave)}$ = 9.5 cm/s, with corresponding $F:u_{(ave)}$ values of 3.6 and 0.26 cm^{-1} (Table I).

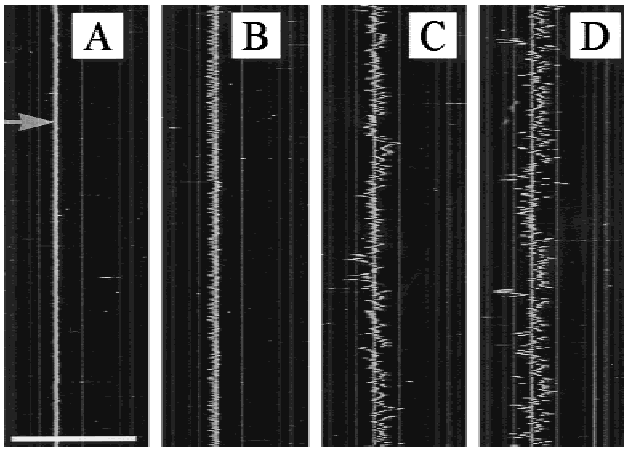

Figure 5. Time trace of streamer displacement (shown by arrow) at various $u_{(ave)}$; (A) 4.7, (B) 9.5, (C) 11.3, and (D) 16 cm/s. The time traces were made by repeatedly scanning the line shown in Figure 2A that intersected the streamer indicated in the same figure. The X axis represents distance and the Y axis time. The negative of the original image is shown for clarity. Scale bar = 500 μm.

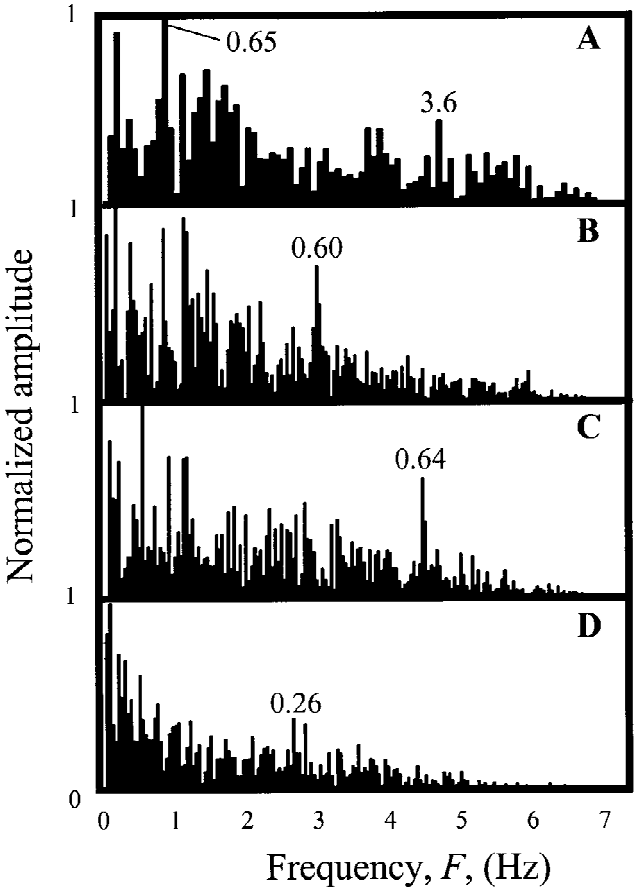

Figure 6. Power spectra of oscillatory streamer motion generated from fast Fourier transform analysis of the time trace data at various $u_{(ave)}$; (A) 1.2, (B) 4.7, (C) 6.9, and (D) 9.5 cm/s. Isolated peaks were identified by eye and are shown with their associated frequency to flow velocity ratio (cm^{-1}).

The amplitude [half of the maximum range of lateral (X–Y) motion], was measured at a point of 1375 μm along a 1440-μm long streamer (Fig. 2A). The amplitude increased in a sigmoidal shaped curve with increasing $u_{(ave)}$ (Fig. 7). Initially the amplitude increased slowly from 0 μm at no flow to 5 μm at $u_{(ave)}$ = 4.7 cm/s. At $u_{(ave)}$ greater than 4.7 cm/s, the amplitude increased more rapidly until a maximum value of approximately 250 μm was reached at a $u_{(ave)}$ of 29 cm/s. The amplitude then stayed approximately the same up to the maximum $u_{(ave)}$ of 50.5 cm/s.

Table I. Relationship between average flow velocity ($u_{(ave)}$) and frequency (F) of streamer oscillation.

$u_{(ave)}$ (cm/s)	F (Hz)	$F:u_{(ave)}$ ratio (cm^{-1})
1.2	0.78	0.65
1.2	4.3	3.6
4.7	2.8	0.60
6.9	4.2	0.64
9.5	2.5	0.26

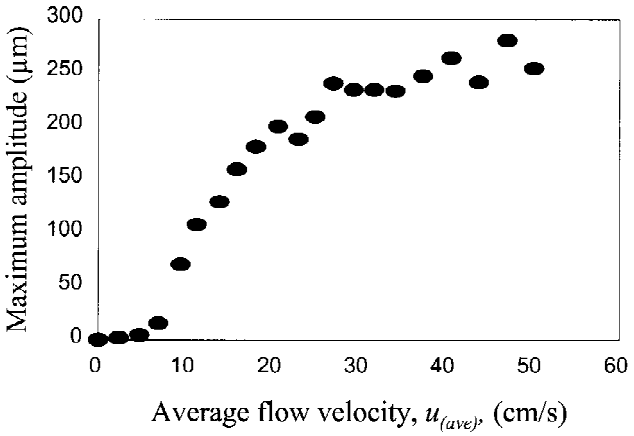

Figure 7. The maximum amplitude of the biofilm streamer shown in Figure 2A increased with $u_{(ave)}$ in a sigmoidal shaped curve.

DISCUSSION

The relationship between ΔP and $u_{(ave)}$ in the clean flow cell indicated that flow was turbulent when $u_{(ave)}$ was 18 cm/s (Re 1192) (Fig. 1). The velocity exponent (m) was 1.84, which was within the established range for turbulent flow over various surfaces (Fox, 1974). After 7 days the biofilm was composed of cell clusters, most of which had developed streamers from the trailing edge, and surrounding water channels. The streamers were flexible as evidenced by their oscillatory motion in the flow stream.

Influence of Biofilm on Pressure Drop and Energy Loss Coefficient (k)

As the biofilm developed, the pressure drop across the flow cell increased in a sigmoidal curve similar to that described previously (Characklis, 1979; Picologlou et al., 1980). The k measured across the flow cell colonized with biofilm was 2.2 times greater than the k measured across the clean flow cell. Because the flow cell geometry remained constant, the additional energy losses can be attributed to the drag caused by the biofilm.

Because k is easily obtained from velocity–pressure drop data, independent of velocity and readily understood by engineers, it is a useful parameter for comparing energy losses in pipe fittings with and without biofilm. However, because loss coefficients will be specific to particular plant components and will depend on the pipe configuration, the influence of biofilm growth should be assessed individually. In pipelines where pumping costs are significant, an increase of only a few percent could be important; but the effect of this will depend on the relative significance of pipe friction and change of altitude along the line.

Biofilm Thickness

In previous work a possible link was observed between the thickness of the biofilm with respect to the thickness of the viscous sublayer and increased pressure drop. In our experiments at the highest flow velocity (50.5 cm/s) the thickness of the viscous sublayer (δ_v) (calculated for a smooth tube) was approximately 280 μm (Characklis et al., 1990),

$$\delta_v = \frac{10\,D_h}{\mathrm{Re}}\left(\frac{f}{2}\right)^{-0.5}. \qquad (5)$$

This is over 3 times greater than the height of the largest cell clusters in our biofilm (85 μm). This finding does not support earlier work that reported that the biofilm only caused an increase in pressure drop when the biofilm thickness was equal to that of the viscous sublayer (Bryers and Characklis, 1981; Characklis, 1979; McCoy and Costerton, 1982; McCoy et al., 1981; Picologlou et al., 1980). However, many of their thickness measurements were based on volume displacement and therefore represented an average. The proportion of surface area covered by our biofilm was approximately 42%; if their biofilms were similar, the height of the largest patches of biofilm may have been underestimated.

Biofilm Surface Coverage

Time dependent factors other than biofilm thickness may be more significant to the onset of increased energy loss. It has been shown that surface coverage and pattern of surface protrusions can influence the drag effects of such protrusions (Massey, 1979; Vogel, 1994). The surface coverage of our biofilm (42%) was much greater than the 8.3% (1/12) reported by Nowell and Church (1979) that was required for the onset of high flow resistance skimming flow. However, the height and diameter dimensions of the cell clusters ranged between 1 and 2 orders of magnitude. Because the larger surface protrusions can have a dominant influence on overall roughness, the effective roughness coverage may be less.

Streamer Oscillations and Vortex Shedding

Oscillation Frequency

The relationship between the frequency of streamer oscillation and flow velocity was investigated to determine if the streamer motion could be attributed to vortex shedding and, hence, related to drag. Only frequencies below approximately 6.7 Hz could be measured due to limitations of the data capture (scan) rate. The frequency to velocity ratio of the data with the best defined amplitude peaks ($u_{(ave)}$ = 1.2, 4.7, and 6.9 cm/s) were similar (0.65, 0.60, and 0.64 cm^{-1}, respectively), indicating a direct relationship between velocity and frequency (Fig. 6). Two other identified peaks had $F{:}u_{(ave)}$ ratios of 3.6 and 0.26 cm^{-1} ($u_{(ave)}$ = 1.2 and 9.5 cm/s, respectively). All of the $F{:}u_{(ave)}$ ratios were close to multiples of 0.3 and may represent harmonics of a dominant frequency. The Strouhal number (St),

$$\mathrm{St} = \frac{l_{ch}\,F}{u} \qquad (6)$$

(where l_{ch} is a characteristic length, such as the object diameter), is a dimensionless parameter used to predict the expected frequency of shedding of an object in a flow stream (Vogel, 1994). The St for rigid cylinders is known to be approximately 0.2 over a wide range of Re (10^2–10^5). Of more relevance to this study, Nakata and Ohba (1996) reported that the St for elastoflexible cylinders is also close to 0.2. Therefore, for a given body the frequency of vortex shedding may be considered directly proportional to flow velocity over a wide range of velocities.

Because the oscillation frequency of the biofilm streamers appeared to be directly related to $u_{(ave)}$, we concluded that the streamer oscillations were likely caused by the vortices shed from the upstream cell clusters to which they were attached. However, our frequency measurements were limited to 6.7 Hz and periodicity was only detected for velocities up to 9.5 cm/s. Possibly at these lower flow velocities the flow was in the isolated roughness regime where streamer motion may be predictable. However, at higher flow velocities there may be wake interaction flow in the biofilm region. In this case flow will be a complex, possibly chaotic, interaction of wakes and the vortex shedding of each wake would be a function of the cluster diameter and local flow velocity. Because the cell clusters have a range of diameters and consequently a range of local Re based on cluster diameter, we should expect that as velocity increases, eddies are initially generated behind larger clusters. However, at higher velocities all clusters will shed eddies.

Oscillation Amplitude

The amplitude of streamer motion was a function of the flow velocity (Fig. 7). At low flow there was very little motion. However, there was a rapid increase in amplitude when $u_{(ave)}$ was increased to 9.5 cm/s. The amplitude continued to steadily increase with $u_{(ave)}$ until a plateau was reached at approximately 30 cm/s. The sigmoidal shape of the amplitude–velocity curve can be explained by hydrodynamics at the low flow velocities and biofilm material properties at the high flows. At low flow rates viscous forces predominate and any eddies shed from the clusters are quickly dampened. However, vortex shedding occurs when momentum forces begin to predominate. The vortices, which are alternately shed from each side of the cluster, push against the streamer causing it to oscillate from side to side. Displacement may be limited by the flexibility of the biofilm material.

Biofilm Sloughing and Streamer Failure

When the shear stress (τ_w) at the wall of the flow cell was 1.32 N/m^2 ($u_{(ave)}$ = 50.5 cm/s), some cell clusters were sloughed off and some of the streamers broke away. In the area of the detached clusters there were still thin pieces of biofilm attached to the glass, indicating that the bonds between the base film and the glass substratum were stronger than the internal cluster bonds. Many of the streamers also broke away, even though the clusters remained attached. Presumably this occurred when the drag force on the streamer exceeded the strength of the streamer material.

Concluding Remarks

We believe that the work reported in this article is an important step toward a greater understanding of the complex interactions between flowing water and filamentous, flexible biofilms. We can use the biofilm itself as a flow indicator and by quantifying streamer oscillations, we can relate such oscillations to vortex generation and drag. However, further research is required to fully elucidate the influence of biofilm streamers on drag in a system. Although it is assumed that the streamers cause an increase in drag, this is not necessarily the case. Biofilm filaments have a relatively high surface area to volume ratio that would cause an increase in skin drag. However, this may be less important than their effect on pressure drag in the high flows in which they grow. The streamers may reduce drag by making the biofilm clusters more streamlined. Alternatively, streamer oscillations may merely reflect the vortices shed by the clusters, regardless of their presence. The elastic nature of the biofilm polymer may contribute (along with water viscosity) to vortex dampening, thus reducing the drag. Finally, it would be interesting, but technically very difficult, to selectively remove biofilm streamers and determine the relative contributions of the cell clusters and the streamers on measured energy losses.

CONCLUSIONS

1. Filamentous biofilm streamers formed from the trailing edge of cell clusters in turbulent flow.
2. The loss coefficient k was a useful comparative measure of the influence of biofilm colonization on energy losses across the flow cell.
3. The k measured across a biofilm colonized flow cell was more than twice that across a clean flow cell.
4. Biofilm streamers were flexible and oscillated in the flowing water.
5. In our range of measurable frequencies (0.12–6.7 Hz), the frequency of streamer oscillation was directly proportional to the flow velocity, suggesting that streamer oscillations were caused by vortex shedding from the cell clusters.
6. Streamer displacement increased as a function of flow velocity in a sinusoidal curve. A maximum displacement was reached at a flow velocity of 30 cm/s (Re 1986).

The research was supported in part by the cooperative agreement EEC-8907039 between the National Science Foundation and Montana State University. For their technical advice we thank: Trevor Priest and Fred Flack from the Department of Physics and Christopher Jones from the Department of Mathematics, Exeter University; Al Cunningham, the Center for Biofilm Engineering at Montana State University; and Dirk deBeer, Max Planck Institute of Marine Microbiology, Bremen.

NOMENCLATURE

Dimensions in terms of mass (M), length (L), and time (T) are in parentheses.

D_h	hydraulic diameter (L)
f	friction factor (dimensionless)
F	frequency ($/T$)
k	loss coefficient (dimensionless)
l_{ch}	characteristic length (L)
Q_R	flow rate in the recycle loop (L^3/T)
m	flow velocity exponent (dimensionless)
n	sample number
r^2	regression correlation coefficient (dimensionless)
Re	Reynolds number (dimensionless)
Re_r	roughness Reynolds number (dimensionless)
St	Strouhal number (dimensionless)
u	flow velocity (L/T)
$u_{(ave)}$	average flow velocity (L/T)
ΔP	pressure drop ($M/L/T^2$)
δ_v	thickness of the viscous sublayer (L)
θ	hydraulic residence time (T)
ρ_w	density of water (M/L^3)
τ_w	wall shear stress ($M/L/T^2$)
ν	kinematic viscosity (L^2/T)

References

Bryers, J., Characklis, W. G. 1981. Early fouling biofilm formation in a turbulent flow system: Overall kinetics. Water Res. **15**: 483–491.

Characklis, W. G. 1979. Biofilm development and destruction in turbulent flow. Presented at the Annual Cooling Tower Institute Meeting, Houston, TX, January 1979.

Characklis, W. G., Turakhia, M. H., Zelver, N. 1990. Transport and interfacial transfer phenomena, pp. 265–340. In: W. G. Characklis and K. C. Marshall (eds.), Biofilms. Wiley, New York.

deBeer, D., Stoodley, P., Lewandowski, Z. 1994b. Liquid flow in heterogenous biofilms. Biotechnol. Bioeng. **44**: 636–641.

deBeer, D., Stoodley, P., Roe, F., Lewandowski, Z. 1994a. Effects of biofilm structures on oxygen distribution and mass transfer. Biotechnol. Bioeng. **43**: 1131–1138.

Fox, J. A. 1974. An introduction to engineering fluid mechanics. Macmillan Press Ltd., London.

Jumars, P. A., Nowell, A. R. M. 1984. Fluid and sediment effects on marine benthic community structure. Am. Zool. **24**: 45–55.

Kay, J. M. 1957. Fluid mechanics and heat transfer. Cambridge University Press, New York.

Lewandowski, Z., Stoodley, P. 1995. Flow induced vibrations, drag force, and pressure drop in conduits covered with biofilm. Water Sci. Technol. **32**: 19–26.

Lewandowski, Z., Stoodley, P., Altobelli, S. 1995. Experimental and conceptual studies on mass transport in biofilms. Water Sci. Technol. **31**: 153–162.

Massey, B. S. 1979. Mechanics of fluids, 4th edition. Van Nostrand Reinhold Company, New York.

McCabe, W. L., J. C. Smith. 1976. Unit operations of chemical engineering, 3rd edition, Chemical engineering series. McGraw–Hill, New York.

McCoy, W. F., Bryers, J. D., Robbins, J., Costerton, J. W. 1981. Observations of fouling biofilm formation. Can. J. Microbiol. **27**: 910–917.

McCoy, W. F., Costerton, J. W. 1982. Fouling biofilm development in tubular flow systems. Dev. Ind. Microbiol. **23**: 551–558.

Nakata, M., Ohba, K. 1996. Increases in vortex shedding frequency from an elasto-flexible cylinder in uniform water flow. J. Phys. Soc. Jpn. **65**: 3080–3081.

Nowell, A. R. M., Church, M. 1979. Turbulent flow in a depth limited boundary layer. J. Geophys. Res. C: Oceans Atmos. **84**: 4816–4824.

Picologlou, B. F., Zelver, N., Characklis, W. G. 1980. Biofilm growth and hydraulic performance. J. Hydraul. Div. Am. Soc. Civ. Eng. **106**(HY5): 733–746.

Stoodley, P., deBeer, D., Lewandowski, Z. 1994. Liquid flow in biofilm systems. Appl. Environ. Microbiol. **60**: 2711–2716.

Vogel, S. 1994. Life in moving fluids, 2nd edition. Princeton University Press, Princeton, NJ.